

# Quantitative Mapping of Endosomal DNA Processing by Single Molecule Counting

Ved Prakash, Konstantinos Tsekouras, Muthukumaran Venkatachalapathy, Laurie Heinicke, Steve Pressé, Nils G. Walter,\* and Yamuna Krishnan\*

**Abstract:** Extracellular DNA is engulfed by innate immune cells and digested by endosomal DNase II to generate an immune response. Quantitative information on endosomal stage-specific cargo processing is a critical parameter to predict and model the innate immune response. Biochemical assays quantify endosomal processing but lack organelle-specific information, while fluorescence microscopy has provided the latter without the former. Herein, we report a single molecule counting method based on fluorescence imaging that quantitatively maps endosomal processing of cargo DNA in innate immune cells with organelle-specific resolution. Our studies reveal that endosomal DNA degradation occurs mainly in lysosomes and is negligible in late endosomes. This method can be used to study cargo processing in diverse endocytic pathways and measure stage-specific activity of processing factors in endosomes.

Macrophages are innate immune cells that endocytose single- and double-stranded DNA through scavenger receptors. Endocytosed DNA cargo is trafficked along the endolysosomal pathway, progressing from the early endosome to the late endosome, finally reaching the lysosome where it is degraded. The stage-specific processing of endocytic cargo has important implications for pathogen evasion of the immune system, antigen cross-presentation, as well as in differentiating “self” i.e., molecules of host origin, and non-self, i.e., molecules of foreign or pathogenic origin.<sup>[1–3]</sup> DNA is distinguished as self or non-self by host immune cells based on their relative rates of digestion in endocytic organelles.<sup>[2]</sup>

Immunogenic CpG-containing DNA (CpG-DNA) is processed in endolysosomes of dendritic cells by DNase II such that the digestion-resistant DNA fragments activate Toll-like receptor-9 (TLR-9).<sup>[4]</sup> However, it is still unclear in which organelle these processes occur owing to the paucity of quantitative assays in cargo processing while retaining organelle-specific localization information. Endosomal processing is mainly studied using biochemical assays such as sulfation, radio labeling, RT-PCR, and transient or induced protein expression.<sup>[5–8]</sup> While these methods quantitate cargo processing in cell extracts, organelle-specific spatial information cannot be obtained. In contrast, fluorescence microscopy provides organelle-specific spatial information but without the ability to quantitate endocytosed cargo.<sup>[5,9,11,12]</sup> Although super-resolution microscopy has been used to quantitate marker proteins in organelles,<sup>[13,14]</sup> one still cannot quantitatively map the processing of endocytic cargo.

Herein, we have developed a method to count endosomal cargo by photobleaching upon targeting fluorescently labeled DNA to specific subcellular compartments.<sup>[15]</sup> Photobleaching has been used to count cytosolic microRNA copy number.<sup>[16]</sup> Herein, we expand this concept to include organelle-specific information and thereby address cargo processing by developing a method called organellar single-molecule, high-resolution localization and counting (oSHiRLoC). Using oSHiRLoC, we combine the molecular precision afforded by synthetic DNA reporters, spatial information provided by fluorescence microscopy, and the quantitative information yielded by photobleaching-based counting to map the DNase II-mediated DNA processing along the endolysosomal pathway.

In order to construct organelle specific maps of endosomal DNA processing, we incubated (a “pulse” step) alveolar macrophages J774A.1 cells with a 57-base pair double-stranded (ds)DNA reporter cargo labeled with Alexa 488 (dsDNA-A488) in 19 mole equivalents excess of a reference tracer, i.e., the same dsDNA sequence labeled with Cy5 fluorophore (dsDNA-Cy5) (Figure 1a). These sequences were chosen based on previously reported sensors from our lab for the detection of various analytes.<sup>[17–20]</sup> Cells were washed, incubated for a specified duration (a “chase” step), fixed and imaged using total internal reflection fluorescence (TIRF) microscopy. The brighter, more photostable Alexa488 channel was used as a fiducial marker of the endocytic compartment; while the Cy5 channel was used to generate photobleaching reporter time traces, leveraging the low cellular autofluorescence in this channel (Figure 1b). Given the TIRF penetration depth of circa 250 nm, approximately 52 % of early endosomes ( $n = 6$  cells), 37 % of late

[\*] Dr. L. Heinicke, Prof. N. G. Walter  
Single Molecule Analysis Group, Department of Chemistry  
University of Michigan  
Ann Arbor, MI 48109-1055 (USA)  
E-mail: nwalter@umich.edu

Dr. V. Prakash, Dr. M. Venkatachalapathy, Prof. Y. Krishnan  
Department of Chemistry, University of Chicago  
Chicago, IL 60637 (USA)  
E-mail: yamuna@uchicago.edu

Prof. Y. Krishnan  
Grossman Institute of Neuroscience, Quantitative Biology and  
Human Behavior, University of Chicago  
Chicago, IL 60637 (USA)

Dr. K. Tsekouras, Prof. S. Pressé  
Department of Physics and School of Molecular Sciences  
Arizona State University  
Tempe, AZ 85287 (USA)

Supporting information and the ORCID identification number(s) for the author(s) of this article can be found under:  
<https://doi.org/10.1002/anie.201811746>.

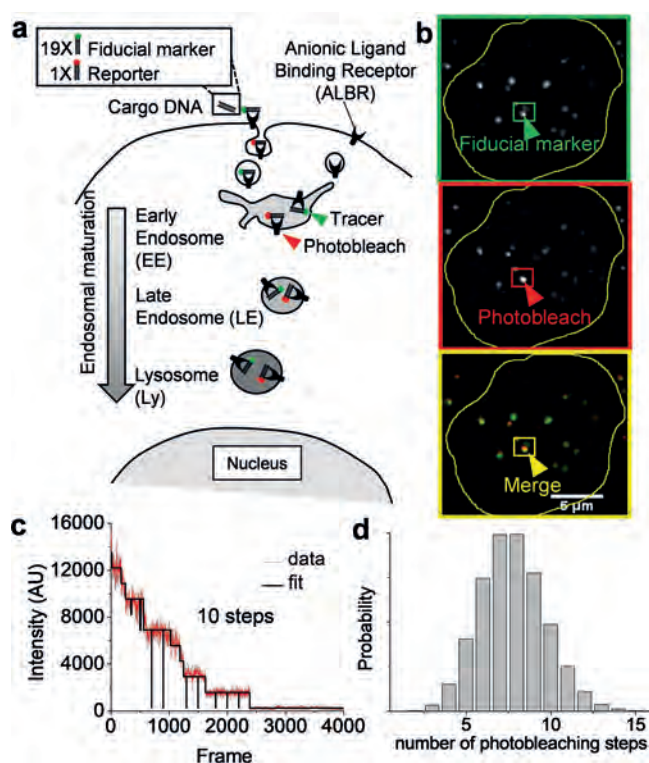


**Figure 1.** Work flow for counting the number of cargo DNA molecules in endosomes of J774 cells. a) Schematic of a cell labeled with a 19:1 ratio of dsDNA-A488 (fiducial marker)/dsDNA-Cy5 (reporter) along the endolysosomal pathway. b) Representative TIRF image of early endosomes (EE) of J774A.1 cells labeled with cargo DNA cocktail imaged in Alexa 488 channel and Cy5 channel. c) Representative photobleaching steps measured in Cy5 channel for the highlighted endosome. d) Histogram of number of photobleaching steps observed for  $n=200$  lysosomes. Number of devices per compartment = number of photobleaching steps observed  $\times$  dilution factor.

endosomes ( $n=5$  cells), and 23% of lysosomes ( $n=5$  cells) were found to be illuminated. To eliminate artefacts arising from autofluorescence, only those compartments with both Alexa 488 and Cy5 signal were analyzed. Since both DNA probes have identical sequences, and scavenger receptors take up dsDNA mainly based on the overall negative charge,<sup>[17]</sup> uptake efficiency and organelle localization is expected to be similar, with all organelles showing similar ratios of Cy5/Alexa488 labels (Supporting Information, Figure S9). Cy5-labeled ssDNA was not retained in endosomes, either owing to its rapid degradation or endosomal translocation.<sup>[21]</sup> This worked in our favor, creating a clean system to report on the abundance of dsDNA cargo, which does not undergo endosomal translocation.<sup>[15]</sup> We then extracted the number of photobleaching steps for every Cy5 time-trace (Figure 1c and Supporting Information, Figure S7). The average number of DNA duplexes in a given compartment could then be calculated from the product of the number of photobleaching steps observed and the probe dilution factor, i.e., the ratio of dsDNA-A488 to dsDNA-Cy5 (Figure 1d).

To assign cargo DNA molecules to specific stages of endosomal maturation, we standardized pulse and chase times for cargo DNA to reach the early endosome, the late

endosome, and the lysosome in J774A.1 cells. Using transferrin-rhodamine B as a marker for early/sorting endosomes,<sup>[19,20]</sup> we found maximal colocalization of transferrin-rhodamine B (500 nm) and cargo DNA (500 nm) in early endosomes (Figure 2a,d) and no colocalization in late endosomes and lysosomes for a 10 min pulse followed by a circa 5–10 min chase (Supporting Information, Figure S1). Similarly, ovalbumin marks late endosomes in J774A.1 cells.<sup>[8]</sup> We found significant cargo DNA colocalization with ovalbumin-FITC with a 10 min pulse and a 30 min chase, highlighting significant localization in late endosomes (Figure 2b,e) and insignificant colocalization in early endosomes and lysosomes (Supporting Information, Figure S2). Finally, for lysosomes, we used dextran-TMR, which is known to mark lysosomes in J774A.1 cells using a 16 h pulse and a 2 h chase. Cells treated with cargo DNA and labeled with dextran-TMR colocalized in lysosomes (Figure 2c,f) and the DNA cargo showed lack of colocalization in early and late endosomes (Supporting Information, Figure S3). Next, we established that extraneously added dsDNA was endocytosed specifically through the scavenger receptor (SR) pathway by using a competition assay.<sup>[17]</sup> We showed that Cy5-labeled cargo dsDNA (termed I4<sub>Cy5</sub>) uptake was outcompeted by a 25-fold excess of maleylated BSA, which targets SRs (Figure 2g).

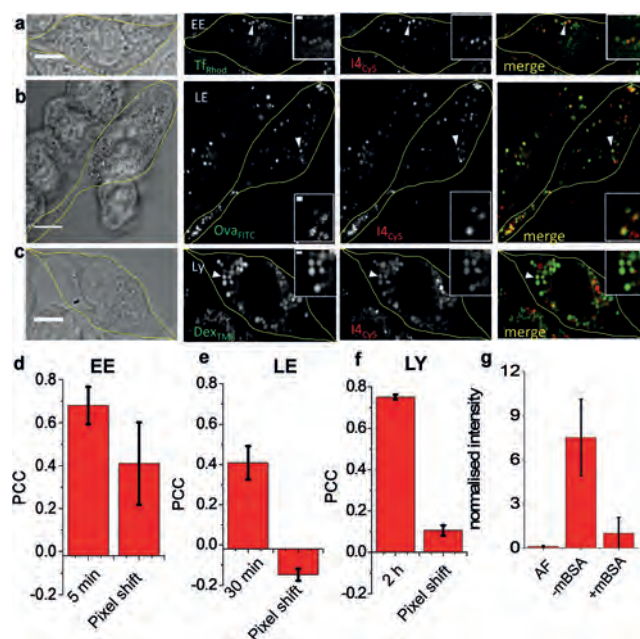


**Figure 2.** Representative single-plane confocal images showing co-localization of cargo with various compartment markers. J774A.1 cells were co-pulsed with dsDNA-Cy5 and a) EE/SE marker transferrin-rhodamine B (TfRhod), b) LE marker ovalbumin-FITC (OvaFITC), and c) lysosomal marker dextran-TMR (DexTMR) followed by 2 h chase. Cell boundaries are demarcated in yellow. d–f) Co-localization (Pearson's correlation coefficient, PCC) between cargo DNA and endosomal markers as a function of chase time in (a–c). Values indicate mean of  $n \approx 20$  cells. g) I4<sub>Cy5</sub> internalization by J774A.1 cells in the presence (+mBSA) and absence (–mBSA) of excess competitor ligand maleylated BSA (mBSA, 10  $\mu$ M) with autofluorescence control (AF). Error bars indicate the mean of independent experiments  $\pm$  s.e.m. ( $n=30$  cells). Scale bars = 10  $\mu$ m and 1  $\mu$ m for inset.



Knowing the time-points of residence of cargo DNA at each stage along the endolysosomal pathway, we mapped cargo DNA abundance as a function of endosomal maturation (Supporting Information, Figure S4). We observed that early endosomes showed two kinds of populations, with endosomes containing circa 200 or circa 700 molecules. Overall, early endosomes showed a mean of  $340 \pm 60$  cargo dsDNA molecules per endosome (Figure 3a, top, green line).

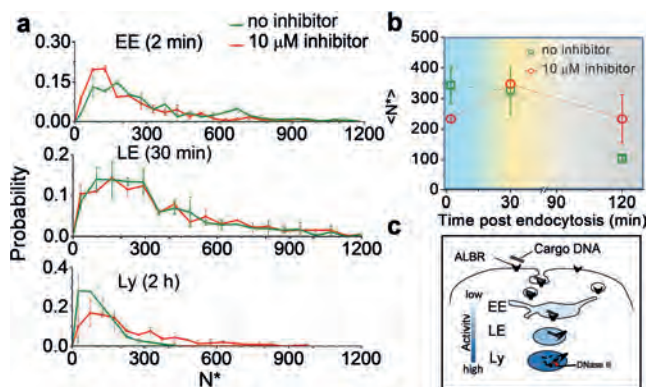


**Figure 3.** Quantitative maps of endosomal DNA processing by single molecule counting. a) Histograms of number of DNA devices observed per compartment in early endosomes (EE, 5 min post endocytosis), late endosomes (LE, 30 min post endocytosis), and lysosomes (Ly, 2 h post endocytosis) in presence and absence of 10 μM DNase II inhibitor within J774A.1 cells. b) Average number of DNA devices per compartment as a function of time. Blue indicates EE, orange indicates LE, and grey corresponds to Ly. Total number of devices per compartment (\*N) = number of photobleaching steps observed × dilution factor.  $n = 200$  endosomes (duplicate) c) Proposed model of DNase II activity in endosomes.

As DNA is endocytosed by clathrin-coated vesicles (ca. 100 nm), we speculate that the population of endosomes showing fewer cargo DNA molecules correspond to these smaller vesicles, while those endosomes showing larger amounts of cargo DNA could correspond to the larger sorting/early endosomes. Late endosomes revealed a fairly broad distribution of cargo DNA abundance with a mean of  $320 \pm 80$  cargo dsDNA molecules per compartment (Figure 3a, middle, green line). Significantly, in lysosomes, the abundance of cargo DNA molecules showed an overall decrease, with most compartments having a mean of  $103 \pm 7$  cargo DNA molecules, indicative of degradation or processing (Figure 3a, bottom, green line).

DNase II is known to be responsible for digestion of endocytosed DNA in macrophages. However, the specific endocytic organelle/s within which it is active is still unknown. To probe for organelle-specific activity of DNase II in immune cells, we treated the cells with a well-characterized specific peptide inhibitor of DNase II, ID2-3, and performed molecule counting experiments at each stage of endosomal maturation (Supporting Information, Figure S5). Upon treatment with a DNase II inhibitor, counting experiments on early endosomes revealed that the mean abundance of cargo dsDNA molecules in early endosomes decreased to  $233 \pm 12$  upon DNase II inhibition (Figure 3b), suggesting a possible

slowdown of endosomal maturation but not uptake. However, single endosome information on cargo abundances revealed that the population containing approximately 200 cargo dsDNA molecules had increased at the expense of the population containing approximately 700 cargo dsDNA molecules ( $P$ -value  $< 0.05$ ). This suggests delayed endosomal maturation and homotypic fusion, as an overall decrease in DNA cargo owing to degradation was not observed. Further, cargo DNA abundance in late endosomes (LE) was not affected by DNase II inhibition (Figure 3a,b). Importantly, when we inhibited DNase II, we observed a significant accumulation of undigested cargo DNA in lysosomes (Ly), showing a mean centered at  $230 \pm 80$  cargo DNA molecules (Figure 3a,b). Interestingly, our statistical data indicate that during DNase II inhibition, cells undergo reduced uptake/trafficking in the early endosomes (Supporting Information, Figure S8). This supports the current hypothesis<sup>[10]</sup> that DNase II-based endosomal DNA processing occurs mainly in lysosomes (Figure 3c).

Furthermore, delayed endosomal maturation as a result of cargo accumulation in lysosomes is also observed in the context of several lysosomal storage disorders, e.g., trafficking of acid sphingomyelinase (ASM) to the lysosome is impeded in ASM knock out cells owing to lysosomal accumulation of sphingomyelin.<sup>[24]</sup> Undigested DNA in endosomes of immune cells comprises one of many important triggers of the immune response. In mice, defective digestion of chromosomal DNA activates phagocytes, leading to anaemia in the embryo and chronic arthritis in adults.<sup>[25]</sup> Digestion of immunogenic CpG DNA in dendritic cells showed that endosomally localized DNase II activity is necessary to trigger TLR-9-mediated cytokine production.<sup>[4]</sup> Loss of DNase II activity results in autoimmune disorders such as systemic lupus erythematosus, for which one of the hallmarks is the production of autoantibodies against dsDNA.<sup>[25,26]</sup> Our capacity to model the immune response using predictive computational models has been hindered by our inability to accurately specify the location and abundance of ligands such as dsDNA that trigger the immune response. The endosomal load of unprocessed dsDNA cargo is a function of the rate of endocytosis, concentration of exogenous dsDNA, receptor density on plasma membrane, and organelle-specific DNase II activity along the endolysosomal pathway.<sup>[4,27]</sup> Current methods to analyze DNA processing quantitate processing efficiency without organelle-specific information or organelle-specific information without the ability to quantitate processing.<sup>[28]</sup>

oSHiRLoC provides quantitative information on cargo DNA processing at organellar resolution. Endosomal cargo quantification using oSHiRLoC is not limited to dsDNA and can be applied to a range of externally added endocytic ligands. It can also be used to assay the location and activity of regulators of endosomal cargo processing. Given the burgeoning use of biologically active, synthetic DNA and RNA nanostructures and circulating endogenous DNA and RNA molecules, methods to understand their differential processing within the cell would be critical to uncover their mechanisms of action. The ability to determine the concentration of immunogens in specific endocytic organelles and correlate these with the strength of the downstream immune

response would enable us to quantitatively model the immune response.

## Acknowledgements

We thank Shareefa Thekkan, Kasturi Chakraborty, Junyi Zou, Aditya Prakash, and Vytas Bindokas for technical assistance and code optimization and Research Computation Center (RCC) at the University of Chicago. We also thank Dr. Sethuramasundaram Pitchiaya, Damon Hoff, and Elizabeth Cameron for initial training. J774A.1 cells were a gift from Prof. Deborah Nelson, Department of Pharmacological and Physiological Sciences, the University of Chicago. S.P. acknowledges support from an NSF CAREER award.

## Conflict of interest

The authors declare no conflict of interest.

**Keywords:** DNA · DNase II · lysosomes · photobleaching · single-molecule counting

**How to cite:** *Angew. Chem. Int. Ed.* **2019**, 58, 3073–3076  
*Angew. Chem.* **2019**, 131, 3105–3108

- [1] M. Rincon-Restrepo, A. Mayer, S. Hauert, D. K. Bonner, E. A. Phelps, J. A. Hubbell, et al., *Biomaterials* **2017**, 132, 48–58.
- [2] G. M. Barton, J. C. Kagan, R. Medzhitov, *Nat. Immunol.* **2006**, 7, 49–56.
- [3] E. B. Compeer, T. W. H. Flinsenbergh, S. G. van der Grein, M. Boes, *Front. Immunol.* **2012**, 3, 37.
- [4] M. P. Chan, M. Onji, R. Fukui, K. Kawane, T. Shibata, S. Saitoh, et al., *Nat. Commun.* **2015**, 6, 5853.
- [5] M. Amessou, V. Popoff, B. Yelamos, A. Saint-Pol, L. Johannes, *Curr. Protoc. Cell Biol.* **2006**, 32, 15.10.1–15.10.21.
- [6] A. Weihe, *Methods Mol. Biol.* **2014**, 1132, 235–243.
- [7] J. J. Sperinde, S. J. Choi, F. C. Szoka, *J. Gene Med.* **2001**, 3, 101–108.
- [8] T. E. Tjelle, A. Brech, L. K. Juvet, G. Griffiths, T. Berg, *J. Cell Sci.* **1996**, 109, 2905–2914.
- [9] Z. Qian, P. G. Dougherty, D. Pei, *Chem. Commun.* **2015**, 51, 2162–2165.
- [10] C. J. Evans, R. J. Aguilera, *Gene* **2003**, 322, 1–15.
- [11] J. A. Brown, R. T. Swank, *J. Biol. Chem.* **1983**, 258, 15323–15328.
- [12] J. Yang, H. Chen, I. R. Vlahov, J.-X. Cheng, *Proc. Natl. Acad. Sci. USA* **2006**, 103, 13872–13877.
- [13] E. M. Puchner, J. M. Walter, R. Kasper, B. Huang, W. A. Lim, *Proc. Natl. Acad. Sci. USA* **2013**, 110, 16015–16020.
- [14] R. Jungmann, M. S. Avendaño, M. Dai, J. B. Woehrstein, S. S. Agasti, Z. Feiger, et al., *Nat. Methods* **2016**, 13, 439–442.
- [15] K. Tsekouras, T. C. Custer, H. Jashnsaz, N. G. Walter, S. Pressé, *Mol. Biol. Cell* **2016**, 27, 3601–3615.
- [16] S. Pitchiaya, L. A. Heinicke, J. I. Park, E. L. Cameron, N. G. Walter, *Cell Rep.* **2017**, 19, 630–642.
- [17] S. Modi, M. G. Swetha, D. Goswami, G. D. Gupta, S. Mayor, Y. Krishnan, *Nat. Nanotechnol.* **2009**, 4, 325–330.
- [18] S. Surana, J. M. Bhat, S. P. Koushika, Y. Krishnan, *Nat. Commun.* **2011**, 2, 340.
- [19] N. Narayanaswamy, K. Chakraborty, A. Saminathan, E. Zeichner, K. Leung, J. Devany, Y. Krishnan, *Nat. Methods* **2019**, 16, 95–102.
- [20] S. Thekkan, M. S. Jani, C. Cui, K. Dan, G. Zhou, L. Becker, Y. Krishnan, *Nat. Chem. Biol.* **2018**, <https://doi.org/10.1038/s41589-018-0176-3>.
- [21] S. Lorenz, S. Tomcin, V. Mailänder, *Microsc. Microanal.* **2011**, 17, 440–445.
- [22] C. I. Raje, S. Kumar, A. Harle, J. S. Nanda, M. Raje, *J. Biol. Chem.* **2007**, 282, 3252–3261.
- [23] S. J. Wadsworth, H. Goldfine, *Infect. Immun.* **2002**, 70, 4650–4660.
- [24] R. Dhami, E. H. Schuchman, *J. Biol. Chem.* **2004**, 279, 1526–1532.
- [25] K. Kawane, H. Fukuyama, G. Kondoh, J. Takeda, Y. Ohsawa, Y. Uchiyama, et al., *Science* **2001**, 292, 1546–1549.
- [26] K. Kawane, K. Motani, S. Nagata, *Cold Spring Harbor Perspect. Biol.* **2014**, 6, a016394.
- [27] C. C. Scott, F. Vacca, J. Gruenberg, *Cell Dev. Biol.* **2014**, 31, 2–10.
- [28] N. Hiroi, V. M. Draviam, A. Funahashi, *Front. Physiol.* **2016**, 7, 196.

Manuscript received: October 16, 2018

Revised manuscript received: January 1, 2019

Accepted manuscript online: January 22, 2019

Version of record online: February 5, 2019

## Supporting Information

### **Quantitative Mapping of Endosomal DNA Processing by Single Molecule Counting**

*Ved Prakash, Konstantinos Tsekouras, Muthukumaran Venkatachalapathy, Laurie Heinicke, Steve Pressé, Nils G. Walter,\* and Yamuna Krishnan\**

anie\_201811746\_sm\_miscellaneous\_information.pdf

## **Author Contributions**

V.P. Conceptualization: Equal; Data curation: Lead; Formal analysis: Lead; Investigation: Equal; Methodology: Lead; Project administration: Supporting; Visualization: Lead; Writing – original draft: Equal

K.T. Formal analysis: Supporting; Software: Supporting

M.V. Writing – original draft: Supporting; Writing – review & editing: Supporting

L.H. Methodology: Supporting

S.P. Funding acquisition: Supporting; Supervision: Supporting

Y.K. Conceptualization: Lead; Data Curation: Lead; Funding acquisition: Lead; Investigation: Lead; Supervision: Lead; Writing - original draft: Lead; Writing - review & editing: Lead

N.W. Conceptualization: Equal; Data curation: Supporting; Funding acquisition: Supporting; Investigation: Supporting; Supervision: Supporting; Writing – review & editing: Supporting.

8      **METHODS**

9      **Materials**

10          All the oligonucleotides used were obtained from Integrated DNA Technologies (IDT). Labeled  
11 oligonucleotides were subjected to ethanol precipitation to remove any contaminating  
12 fluorophores. Peptide inhibitor for DNase II, ID2-3 was procured from Selleckchem.<sup>1</sup>  
13 Oligonucleotides and peptide were dissolved in Milli Q water and was stored at –20°C.

14      **Oligonucleotide sequences used in this study**

Devices	Sequence (5'-3')
dsDNA-488	A488-ATA ACA CAT AAC ACA TAA CAA AAT ATA TAT CCT AGA ACG ACA GAC AAA CAG TGA GTC-3' TAT TGT GTA TTG TGT ATT GTT TTA TAT ATA GGA TCT TGC TGT CTG TTT GTC ACT CAG-5'
dsDNA-Cy5	Cy5-ATA ACA CAT AAC ACA TAA CAA AAT ATA TAT CCT AGA ACG ACA GAC AAA CAG TGA GTC-3' TAT TGT GTA TTG TGT ATT GTT TTA TAT ATA GGA TCT TGC TGT CTG TTT GTC ACT CAG-5'
I4Cy5	Cy5-CCC CTA ACC CCT AAC CCC TAA CCC CAT ATA TAT CCT AGA ACG ACA GAC AAA CAG TGA GTC GAC TCA CTG TTT GTC TGT CGT TCT AGG ATA TAT ATG GGG TTA GGG GTT AGG GGT TAG GGG

15  
16      **Cargo DNA sample preparation**

17          Constituent complementary strands of I4<sub>Cy5</sub> (I4 and I4') were mixed in 20 mM sodium buffer  
18 pH 5.5 containing 100 mM KCl at 5 µM concentration. For dsDNA DNA, constituent strands  
19 dsDNA-Cy5 and I4' or dsDNA-A488 and I4') were mixed at 5 µM concentration in 50 mM  
20 sodium phosphate buffer pH 7. For both cases, the resultant solution was heated from 25°C to 90°C  
21 in 15 min and was then cooled to room temperature at 1°C/2 min and equilibrated at 4°C overnight.

22      **Protein conjugation**

23          Ovalbumin was obtained from Sigma and labeled with FITC using a standard protein labeling  
24 protocol.<sup>2</sup> Briefly, 200 µl of 1.25 mg/ml FITC solution in 0.1 M sodium phosphate buffer at pH 8  
25 was added to 500 µl of 10 mg/ml protein solution. The reaction mixture was adjusted to pH 9.0  
26 with 0.1 M trisodium phosphate. The reaction mixture was maintained at 25°C for 3 hours. Labeled

ovalbumin was purified from reaction mixture using 10 kDa cutoff Amicon filter using PBS and was then stored in PBS at  $-20^{\circ}\text{C}$ .

Mouse Apo-transferrin was obtained from Sigma and was converted to holo-transferrin by loading with Fe(III) as described previously.<sup>3</sup> Briefly, 4.49 mg of  $\text{FeCl}_3$  was dissolved in 2 ml of water and was neutralized with sodium hydroxide. 106 mg of nitrilotriacetic acid was added to it and the solution was neutralized again. 0.5 mg of apo-transferrin was dissolved in 100  $\mu\text{l}$  of buffer 1 (0.1 M  $\text{NaClO}_4$ /20 mM  $\text{NaHCO}_3$ /10 mM Tris-HCl, pH 7.6) (5 mg/ml protein concentration). To this protein solution, 1  $\mu\text{l}$  of above  $\text{Fe}^{3+}$  solution was added, incubated for 1-hr at room temperature and was subjected to 30 kDa cutoff Amicon. Buffer was exchanged with buffer2 (100 mM sodium bicarbonate buffer pH 9) and volume was concentrated to 5 mg/ml.

In order to label holo-transferrin with Rhodamine B, 0.2 ml of 5 mg/ml holo-transferrin solution in pH 9, and 0.1 M sodium bicarbonate buffer was mixed with 6.7  $\mu\text{l}$  of 20 mg/ml Rhodamine B isothiocyanate solution. Solution was allowed to stir at RT for 1 hour and was then subjected to 30 kDa cutoff Amicon purification using perchlorate buffer (0.1 M  $\text{NaClO}_4$ /20 mM  $\text{NaHCO}_3$ /10 mM Tris-HCl, pH 7.6).

#### **Cell culture and labelling with endocytic markers**

J774A.1 macrophages (ATCC No. TIB-67) were a kind gift from Prof. Deborah Nelson, Department of Pharmacological and Physiological Sciences, the University of Chicago. They were cultured in Dulbecco's Modified Eagle's Medium/F-12 (1:1) (DMEM-F12) (Invitrogen Corporation, USA) containing 10% heat inactivated Fetal Bovine Serum (FBS) (Invitrogen Corporation, USA), 100 U/ml penicillin and 100 g/ml streptomycin at  $37^{\circ}\text{C}$  in 5%  $\text{CO}_2$ , and were used at 60% confluence.



In order to label early endosomes, J774A.1 cells were co-pulsed with a cocktail of 1  $\mu$ M Rhodamine labeled holo-transferrin and 500 nM Cy5 labeled dsDNA for 10 min at 37°C. Cells were immediately washed with PBS and placed on ice to prevent endocytosis progression. Cells were surface stripped by incubating them in surface stripping buffer (160 mM sodium ascorbate, 40 mM ascorbic acid, 1 mM  $\text{CaCl}_2$ , and 1 mM  $\text{MgCl}_2$ , pH 4.5.) for 10 min on ice. Cells were then washed with PBS and fixed using 2.5 % paraformaldehyde (PFA) at room temperature for 20 min. For labeling late endosomes, cells were pulsed with Cy5 labeled DNA dsDNA in complete medium for 5 min at 37°C followed by addition of FITC labeled ovalbumin such that its final concentration in pulsing medium was 1  $\mu$ M. After 5 min pulse at 37°C, cells were washed with PBS and were chased at 37°C for 30 min in complete medium. Cells were then washed, surface stripped and fixed as it were done for early endosome sample. For labeling lysosomes, cells were pulsed with 0.5 mg/ml TMR labeled 10 kDa dextran for 16 hours in complete medium at 37°C followed by 2 hours chase in complete medium. Cells were then pulsed with 500 nM Cy5 labeled dsDNA for 10 min followed by 2 hours chase in complete medium. Cells were then washed, surface stripped, fixed and imaged on confocal microscope.

### **Labeling endosomes for molecule counting**

In a typical molecule counting experiment, for labeling early or late endosomes J774A.1 cells were pulsed with a cocktail of 25 nM of dsDNA-Cy5 (reporter) + 475 nM dsDNA-A488 (endocytic tracer) for 10 min and chased for indicated time in DMEM with 0.1% BSA (without serum) at 37°C.

In the same way, lysosomes were labeled with 100 nM of dsDNA-Cy5 (reporter) + 400 nM dsDNA-A488 (endocytic tracer) for no inhibitor sample and with 50 nM of dsDNA-Cy5 (reporter)

+ 450 nM dsDNA-A488 (endocytic tracer) for 10  $\mu$ M inhibitor sample. Cells were then washed with PBS, surface stripped, incubated at room temperature for 3 hours and imaged in imaging buffer (Tris-base 50mM, NaCl 10mM, Glucose 10%, oxygen-scavenging system (0.1 mg/ml glucose oxidase, 0.02 mg/mL catalase, pH=8) on Total Internal Reflection Fluorescence (TIRF) microscope.

### **DNase II inhibitor treatment**

In order to block DNase II activity, J774A.1 cells were pretreated with 10  $\mu$ M DNase II inhibitor peptide ID2-3 in DMEM with 0.1% BSA (without serum) for 1 hour at 37°C.<sup>1</sup> Cells were then pulsed with cargo DNA dissolved in DMEM with 0.1% BSA and 10  $\mu$ M DNase II inhibitor peptide (without serum) at 37°C for 10 min and were chased in DMEM with 0.1% BSA (without serum) and 10  $\mu$ M DNase II inhibitor peptide at 37°C for indicated time.

### **Image acquisition**

Confocal images were acquired Olympus FV1000 confocal laser scanning microscope set up equipped with IX81 body, 60x / NA 1.42 oil (PlanApoN) objective, multi alkali PMTs and laser lines for 488, 543 and 633 nm excitation.

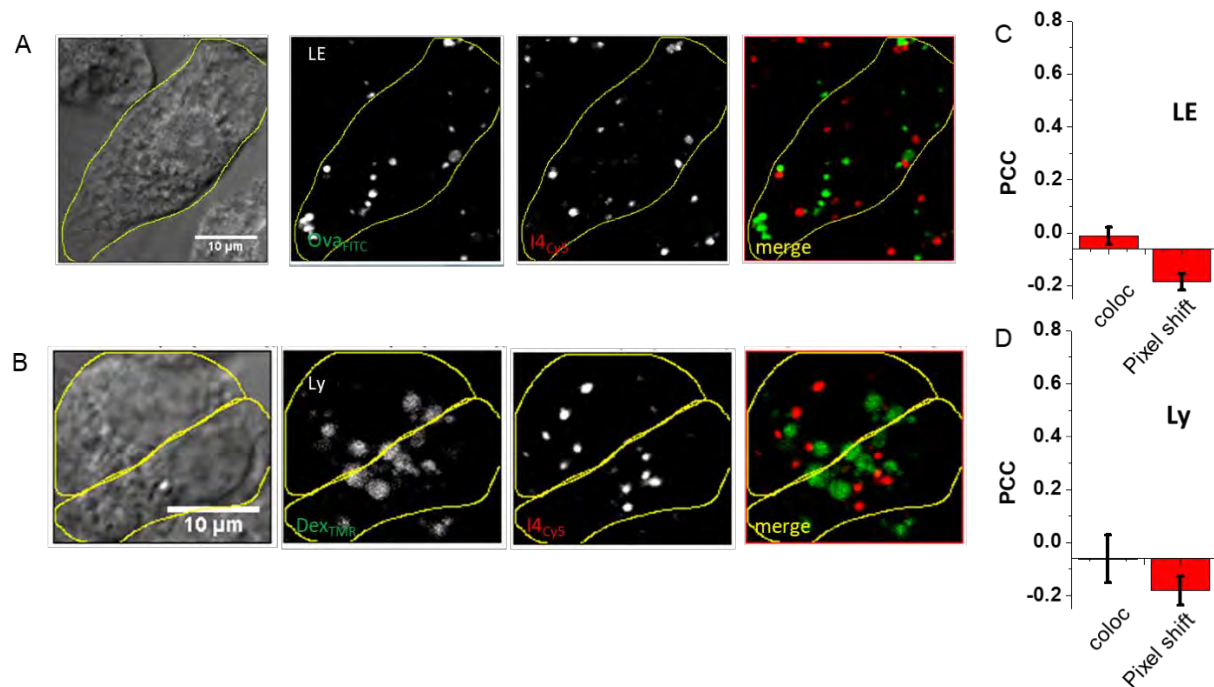
TIRF images for molecule counting were acquired on Leica four-color (405nm, 488nm, 532nm and 642nm) Total Internal Reflection fluorescence (TIRF) microscope equipped with automated critical angle positioning, 160x NA 1.43 state of the art, adhesive-free objective, Suppressed Motion (SuMo) stage which locks in the 160x objective to minimize sample drift and iXon Ultra EMCCD camera. Before image acquisition, samples were allowed to sit on microscope

undisturbed for thermal equilibration. This prevented z-drift during image series acquisition.  
Image series of 4,000 to 12,000 frames was acquired with 100 ms exposure.

## **Image analysis**

J774A.1 cells treated with Cy5 labeled DNA devices labeled various cellular compartments (EE, LE & Ly). Using Fiji, acquired TIRF microscopy slices were used to measure the ratio of number of endosomes in the first plane (closest to coverslip) to the number of endosomes in the entire cell (Converting the image stack into Maximum Z-Projection). In three independent experiments, we detected 51.66% of early endosomes (n=6 cells), 37.34% of late endosomes (n=5 cells) and 23.47% of lysosomes (n=5 cells) illuminated in the first slice of the microscopy image.

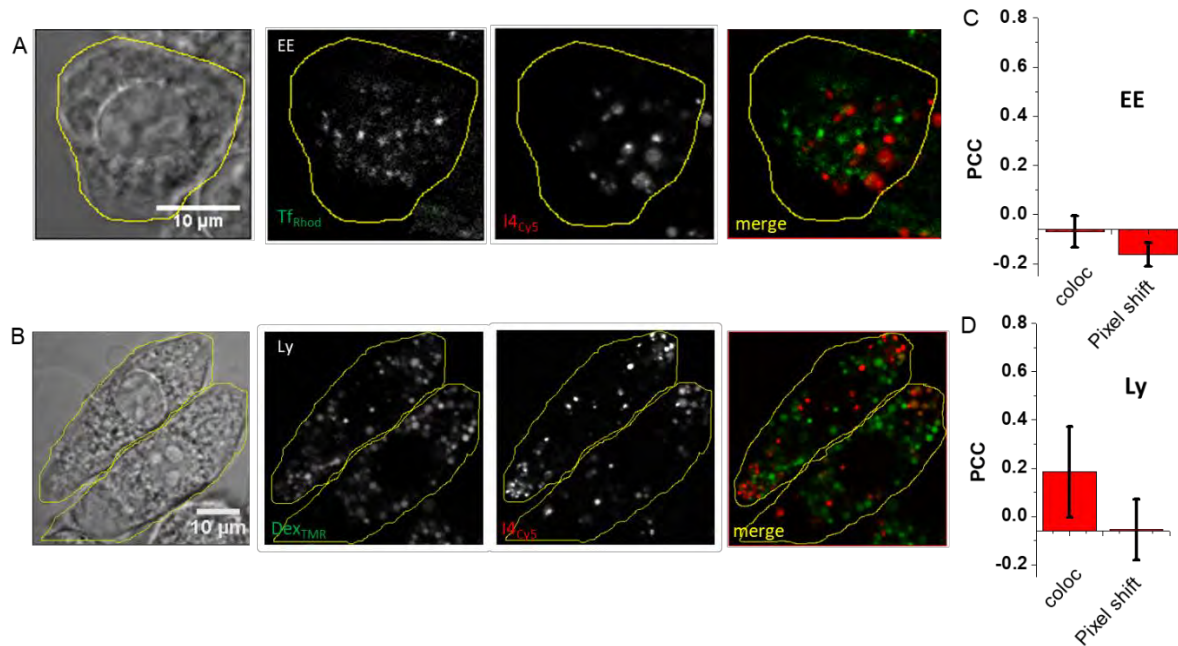
Acquired images were opened in Fiji and were exported into image sets for small areas using custom written ImageJ macro. This was a vital step as too large image sets can't be opened in LabView program due to memory limits. Images were manually analyzed and spots where significant colocalization in endocytic tracer and reporter channels was observed were marked and fluorescence photobleaching trace for each such spot was exported. More than 200 such traces for each sample were then analyzed using the previously reported Python program "Photobleach".<sup>4</sup> Results were then exported into excel and were plotted in OriginPro software.



117

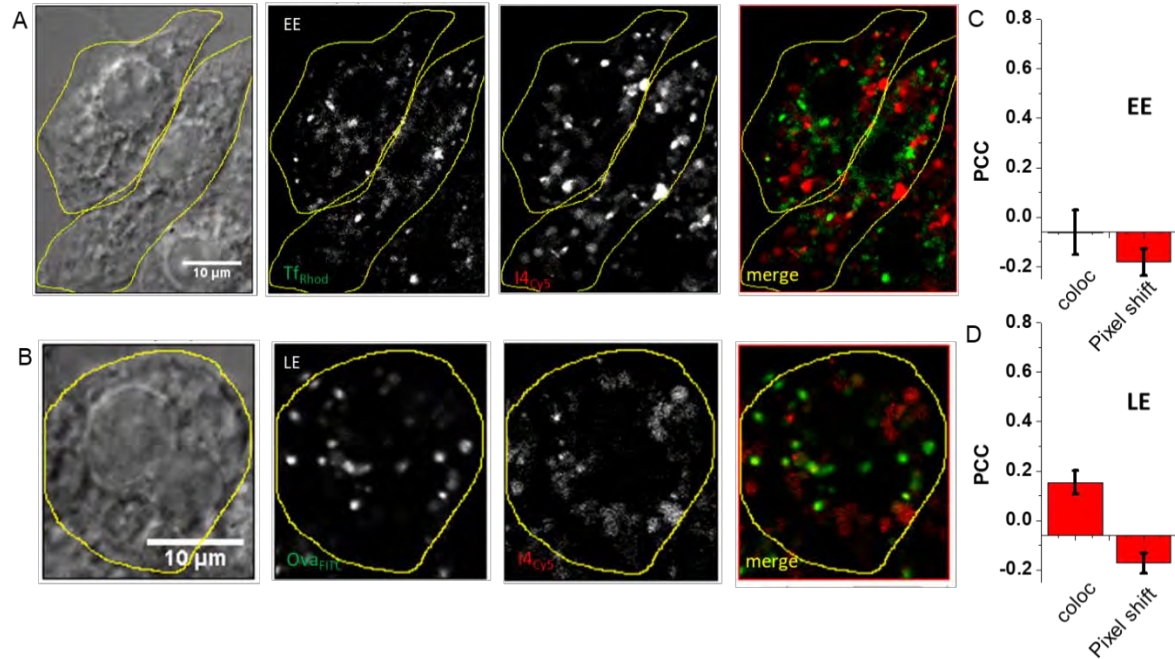
118 **Supplementary Figure S1 | DNA cargo does not co-localize with LE or Ly at 10 min pulse.**

119 *Representative single-plane confocal images showing co-localization of cargo DNA with various*  
 120 *compartment markers at 10 min pulse. (A) J774A.1 cells were pulsed with 500 nM of LE marker*  
 121 *Ovalbumin-FITC (Ova<sub>FITC</sub>) for 5 min followed by a chase of 20 min. These cells were then pulsed*  
 122 *with 500 nM of I4<sub>Cys</sub> for 10 min. (B) Lysosomes were labeled by 16 hours pulse of 0.5 mg/ml*  
 123 *Dextran-TMR (Dex<sub>TMR</sub>) followed by 4 hours chase. These cells were then labeled with I4<sub>Cys</sub> for 10*  
 124 *min. Cell boundaries are demarcated by yellow outlines. (C & D) Quantification of co-localization*  
 125 *between cargo DNA and endosomal markers used in a & b. Values indicate mean of n~20 cells.*

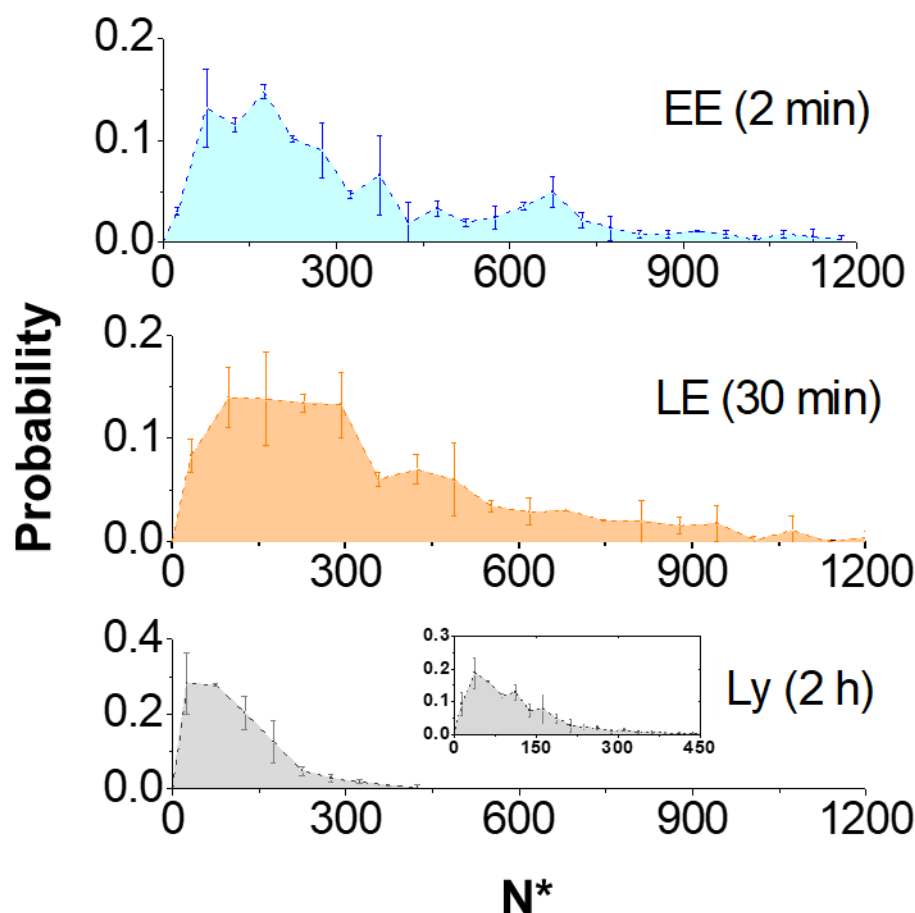


**Supplementary Figure S2 | DNA cargo does not co-localize with EE or Ly at 10 min pulse and 30 min chase.** Representative single-plane confocal images showing co-localization of cargo DNA with various compartment markers at 10 min pulse and 30 min chase. (A) J774A.1 cells were pulsed with 500 nM  $I4_{Cys}$  for 10 min and then chased for 20 min. These cells were labeled with 1  $\mu$ M EE/SE marker transferrin-Rhodamine B ( $Tf_{Rhod}$ ) for 10 min. (B) Lysosomes were labeled by 16 hours pulse of 0.5 mg/ml Dextran-TMR ( $Dex_{TMR}$ ) followed by 3.5 hours chase. These cells were then labeled with  $I4_{Cys}$  for 10 min followed by a chase for 30 min. Cell boundaries are demarcated by yellow outlines. (C & D) Quantification of co-localization between cargo DNA and endosomal markers used in a & b. Values indicate mean of  $n \sim 20$  cells.





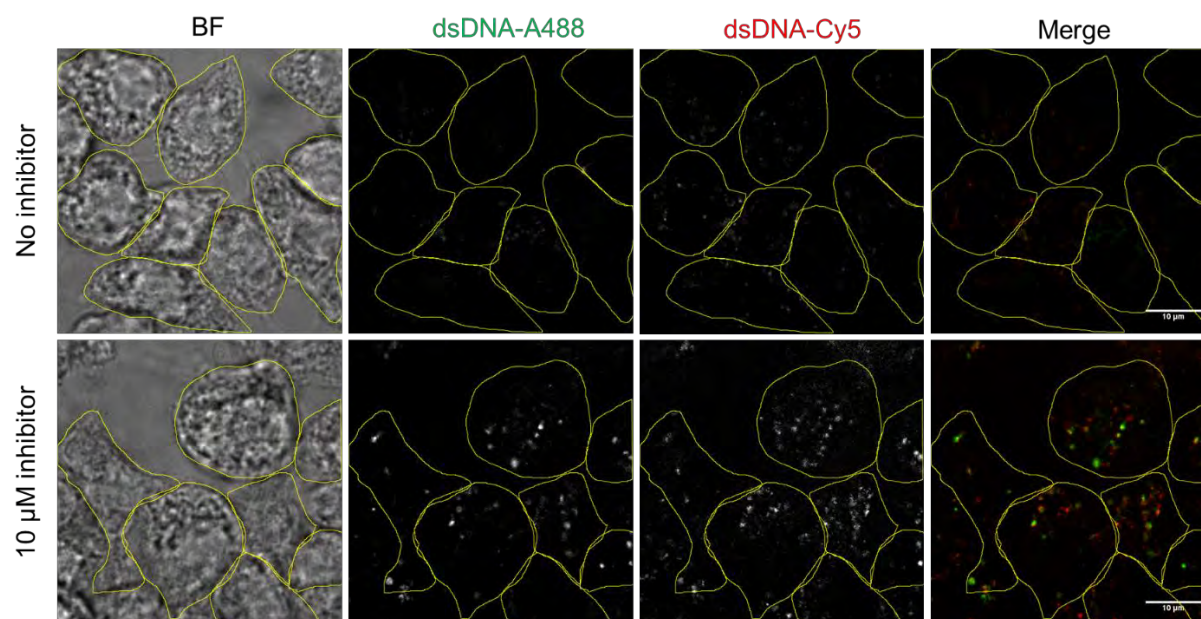
**Supplementary Figure S3 | DNA cargo does not co-localize with EE or LE at 10 min pulse and 2 h chase.** Representative single-plane confocal images showing co-localization of cargo DNA with various compartment markers at 10 min pulse and 2 h chase. (A) J774A.1 cells were pulsed with 500 nM I4<sub>Cy5</sub> for 10 min and then chased for 2 h. These cells were labeled with 1  $\mu$ M EE/SE marker transferrin-Rhodamine B (Tf<sub>Rhod</sub>) for 10 min. (B) J774A.1 cells were pulsed with 500 nM of I4<sub>Cy5</sub> for 10 min followed by a chase for 85 min. These cells were then labeled with 500 nM of Ovalbumin-FITC (Ova<sub>FITC</sub>) for 5 min followed by a chase of 30 min to mark LE. Cell boundaries are demarcated by yellow outlines. (C & D) Quantification of co-localization between cargo DNA and endosomal markers used in a & b. Values indicate mean of n~20 cells.



149

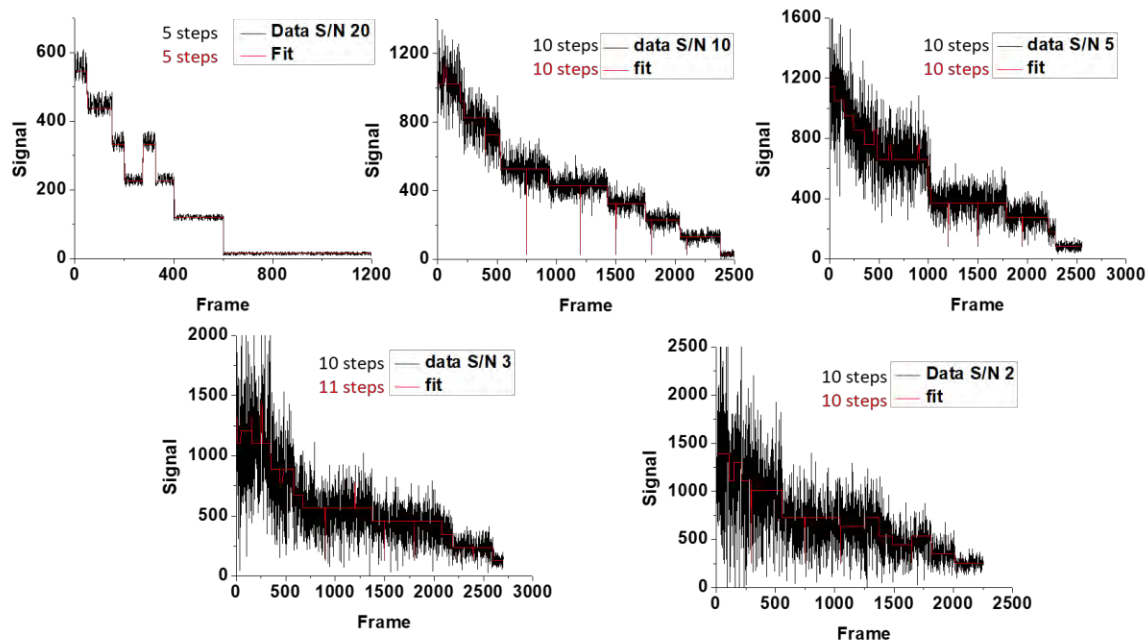
150 **Supplementary Figure S4 / Molecule counting in endosomes.** Histograms of the number of  
 151 devices observed per compartment in early endosomes (EE), late endosomes (LE) and lysosomes  
 152 (Ly) of J774A.1 cells. Early and late endosomes were labeled with 25 nM of dsDNA-Cy5  
 153 (reporter) + 475 nM dsDNA-A488 (endocytic tracer). Lysosomes were labeled with 100 nM  
 154 dsDNA-Cy5 (reporter) + 400 nM dsDNA-A488 (endocytic tracer). Error bars indicate the mean  
 155 of two independent experiments  $\pm$  standard deviation.  $N^* = n_p \times d$  where  $N^*$  = total number of  
 156 devices per compartment,  $n_p$  = number of photobleaching steps observed and  $d$  = dilution factor.  
 157  $n = 200$  endosomes (duplicate). Inset shows a zoom of histogram for lysosome sample with smaller  
 158 bin size showing distribution at lower  $N^*$ .

159



***Supplementary Figure S5 / Effect of DNase II inhibitor on lysosomal cargo DNA processing.***

Lysosomes of J774 cells were labeled with 100 nM of dsDNA-Cy5 (reporter) + 400 nM dsDNA-A488 (endocytic tracer) for no inhibitor sample and with 50 nM of dsDNA-Cy5 (reporter) + 450 nM dsDNA-A488 (endocytic tracer) for DNase II 10  $\mu$ M inhibitor sample. Brightness of red channel image for no inhibitor sample has been scaled to half intensity to compensate for double concentration of dsDNA-Cy5. DNase II inhibitor sample shows bright and large lysosomes.

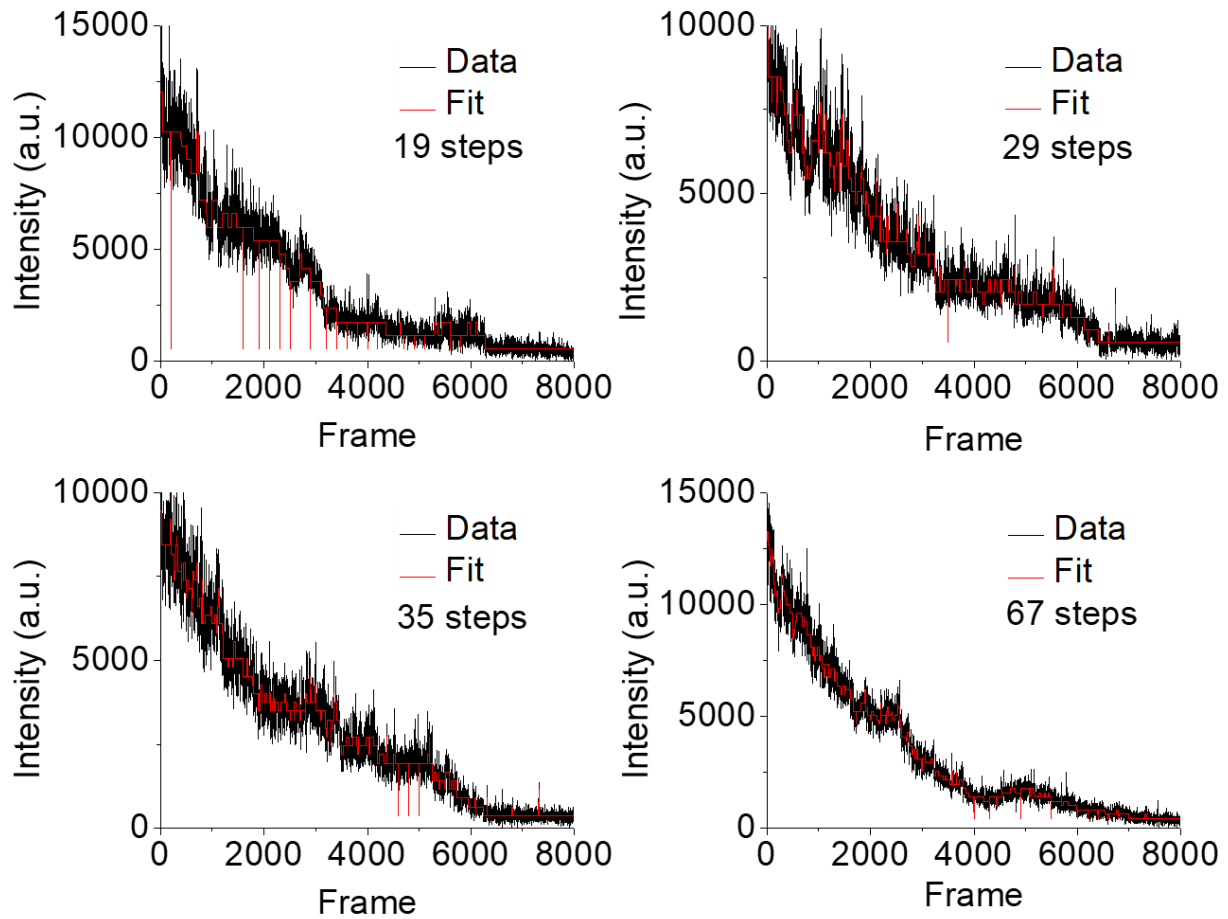


167

168 **Supplementary Figure S6 / Photobleaching software benchmarking.** To test the robustness of  
 169 the algorithm, synthetic photobleaching traces were generated using a MATLAB program for  
 170 various S/N whose steps were detected using the algorithm written by Tsekouras *et al.* Note that  
 171 sharp downward spikes in the fit (see also Fig. S6) are an artifact of the fitting software and can  
 172 be eliminated via a simple post-processing step detailed in the software user guide.

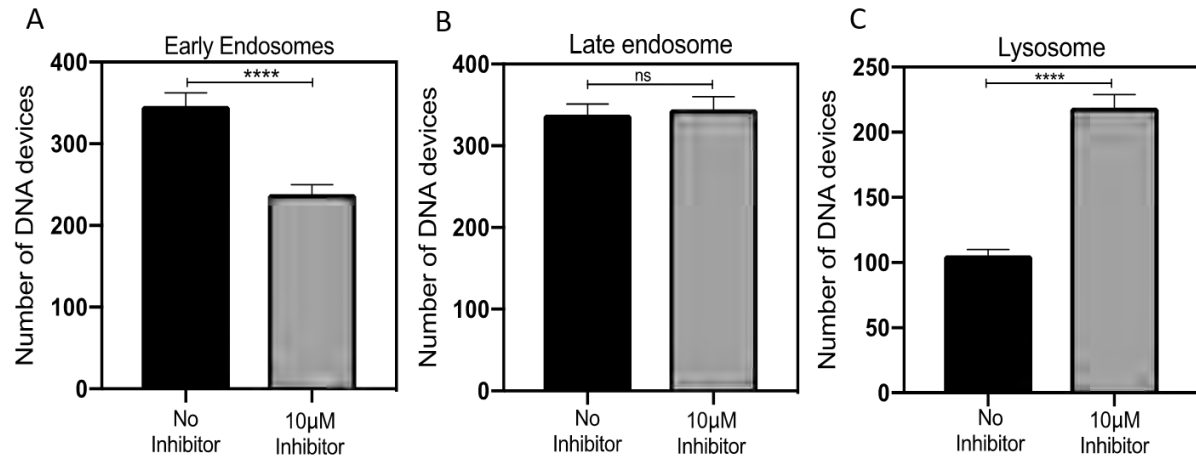
173 Synthetic data = Signal + Poisson noise (fluorophore) + Gaussian noise (detector) + background

174

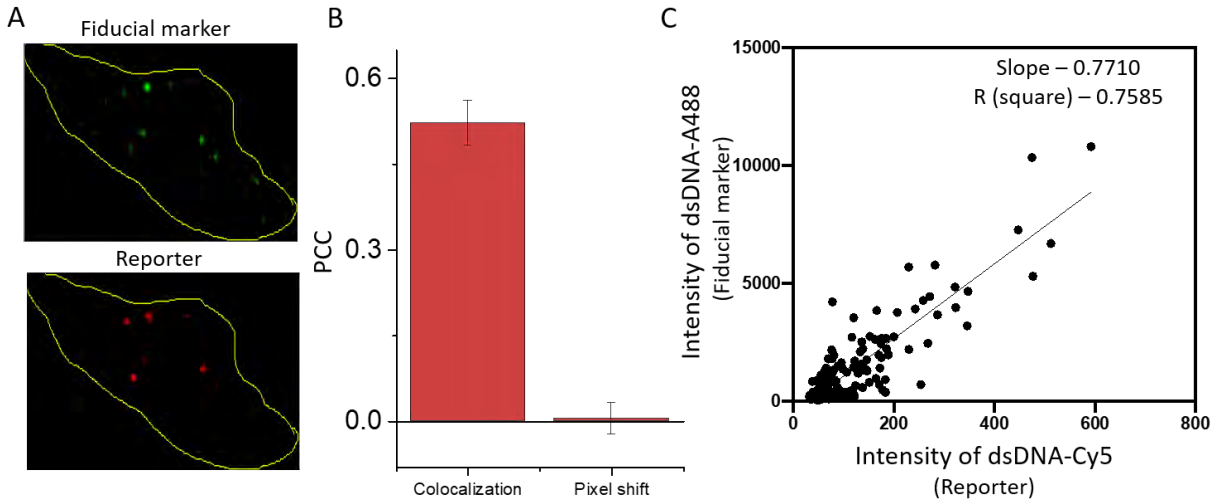


**Supplementary Figure S7/ Photobleaching step detection.** Representative photobleaching decay traces (black) and their detected steps (red) for early endosomes.





**Supplementary Figure S8: Quantification of DNA nanodevices inside endosomal compartments during pharmacological treatment.** Bar graphs of the number of DNA devices in (A) early endosomes (B) late endosomes and (C) lysosomes in the presence (grey) and absence (black) of DNase II inhibitor. \*\*\*\* $p < 0.0001$ , ns = non-significant, where  $p < 0.6139$ .



**Supplementary Figure 9: Quantitative analysis of the DNA devices inside endosomes.** A. Endosomes of J774A.1 cells co labeled with 500nM of dsDNA-488 (Fiducial marker) and dsDNA-Cy5 (Reporter) in 4:1 stoichiometry. B. Pearson Correlation Coefficients (PCC) of colocalized and pixel shifted images of A488 and Cy5 puncta (n=12 cells). C. A plot of intensity in A488 channel versus that in the Cy5 channel per endosome. Black line is a linear fit of the data and the slope and R<sup>2</sup> values are shown.

## REFERENCES

- (1) Sperinde, J. J.; Choi, S. J.; Szoka, F. C. *J Gene Med* 2001, 3, 101–108.
- (2) Mckinney, R. M.; Spillane, J. T.; Pearce, G. W. *J Immunol* 1964, 93, 232–242.
- (3) Bunesco, A.; Besse-Hoggan, P.; Sancelme, M.; Mailhot, G.; Delort, A.-M. *Appl Environ Microbiol* 2008, 74, 6320–6326.
- (4) Tsekouras, K.; Custer, T. C.; Jashnsaz, H.; Walter, N. G.; Pressé, S. *Mol Biol Cell* 2016, 27, 3601–3615.
- (5) Salkind Neil J & Kristin Rasmussen, *Encyclopedia of Measurement and Statistics* (2007), pages 566-567